



# An Al–Si–Ti hierarchical metal–metal composite manufactured by co-spray forming

A.J. Kelly<sup>a,\*</sup>, J. Mi<sup>a</sup>, G.V. Sinha<sup>b</sup>, P. Krug<sup>b</sup>, F. Crosa<sup>c</sup>, F. Audebert<sup>c</sup>, P.S. Grant<sup>a</sup>

<sup>a</sup> Department of Materials, University of Oxford, Parks Road, Oxford, OX1 3PH, UK

<sup>b</sup> PEAK Werkstoff GmbH, Siebenecker Str. 235, Velbert, Germany

<sup>c</sup> Faculty of Engineering, University of Buenos Aires, Av. Paseo Colón 850, Buenos Aires, Argentina

## ARTICLE INFO

### Article history:

Received 21 December 2010

Received in revised form 30 May 2011

Accepted 2 July 2011

Available online 7 July 2011

### Keywords:

Co-spray forming

Metal–metal composite

Extrusion

Accumulated roll-bonding (ARB)

Electron backscattered diffraction (EBSD)

## ABSTRACT

Spray forming with co-injection of a solid particulate phase to form a homogeneous distribution within the final spray formed billet has been studied as a new route to manufacturing metal–metal composites at large scale with negligible oxide. 12 wt%Ti particles were co-injected into an atomised Al alloy droplet spray and co-deposited to form a ~300 kg billet at Peak Werkstoff GmbH, Germany. The microstructure comprised refined equiaxed  $\alpha$ -Al grains (~5  $\mu$ m), spherical Si particles (~1  $\mu$ m) and uniformly distributed Ti particles (~80  $\mu$ m). Sections of the billet were extruded under a range of conditions into long strips 20 mm wide and 6 mm, 2.5 mm and 1 mm thickness. At high strains, the Ti particles were deformed into continuous fibres of a few microns in thickness. The large interfacial area between the fcc  $\alpha$ -Al and hcp Ti inhibited dislocation motion and enhanced tensile properties. Accumulative roll bonding was then performed to higher total strains, while maintaining a constant cross-section, reducing the Ti fibres to sub-micron thickness. The fibres were studied by extraction after selective dissolution of the  $\alpha$ -Al matrix. There was no interfacial reaction between  $\alpha$ -Al and Ti or any measurable oxide formation.

© 2011 Elsevier B.V. All rights reserved.

## 1. Introduction

A metal–metal composite differs from a conventional metal matrix composite in that both the majority matrix and the minority “reinforcing” phase are ductile metals (Russell et al., 2000). The constituent metals generally comprise either a face centred cubic (fcc) metal paired with a body centred cubic (bcc) metal such as Cu–Nb or Al–Nb, or a fcc metal paired with a hexagonal close-packed (hcp) metal such as Al–Ti (Russell et al., 2000). These materials have been manufactured typically by mixing the constituent metals via powder metallurgy (PM) or by co-melting two metals that are miscible as liquid but immiscible as solid so that complete phase separation occurs during solidification. The PM or cast feedstock is then heavily deformed via a series of, or a repetitive process of extrusion, swaging, drawing and/or rolling into wire or sheet form producing an elongated filament morphology in the minority constituent. Metal–metal composites have been studied since the late 1970s when it was discovered by Bevk et al. (1978) that following significant uniaxial deformation processing the resulting strength increased beyond that which can be accounted for by the rule-of-mixtures. The precise mechanism of strengthening in these materials has not been identified unambiguously but the very

large interfacial area between the two crystallographically dissimilar metals is likely to play a central role (Bevk et al., 1978). Ultimate tensile strengths of 2200, 1030 and 890 MPa have been reported for Cu–18 vol%Nb (Bevk et al., 1978), Al–20 vol%Nb (Thieme et al., 1993) and Al–20 vol%Ti (Russell et al., 1999) systems, respectively. Among the severe plastic deformation processes, accumulative roll bonding (ARB) has the advantage of inducing high uniaxial strains without reducing the cross-sectional area (Saito et al., 1999). Therefore, in theory a limitless number of ARB cycles can be imposed although in practice a limit is imposed by the need to remove split material from the strip edges after each cycle.

This paper investigates co-spray forming as a route to manufacturing Al based metal–metal composite feedstock ingots at a scale (~300 kg per billet) significantly beyond previous PM and immiscible alloy system approaches. Furthermore spray forming offers advantages over PM in that significantly fewer oxides are incorporated. Standard extrusion practices are used to deform the billets into strips of different thickness (deformation ratios), followed by accumulative roll-bonding to induce higher strains. Although the Al–Ti system studied here is similar to previous studies by powder metallurgy, e.g. Russell et al. (1999), a much harder disperse third phase of pure Si particles was present in the Al matrix and is suggested to play a role in both the recrystallization behaviour of the  $\alpha$ -Al grains and the deformation of the Ti particles. The novelty of the present work derives from: (1) the demonstration of the feasibility of co-spray forming as a scaled-up manufacturing route for

\* Corresponding author.

E-mail address: [aoife.kelly@materials.ox.ac.uk](mailto:aoife.kelly@materials.ox.ac.uk) (A.J. Kelly).

**Table 1**  
Parameters used for the extrusion of Al–Si + Ti metal–metal composites.

Sample dimension	Extrusion parameters			
	Ratio	True strain	Temperature (°C)	Speed (mm/min)
∅30 mm bar	12	2.5	350	600
2.5 mm × 20 mm strip	162	5.1	380	5.20
1.0 mm × 20 mm strip	408	6.1	415	1.27

metal–metal composites and (2) the use of a third, hard phase to facilitate the required microstructural development.

## 2. Experiments

### 2.1. Spray forming and extrusion

Nominal Al–12 wt%Si alloy with co-injected 12 wt%Ti powder ( $<150 \mu\text{m}$ ,  $D_{50} = 80 \mu\text{m}$ ) was spray formed at Peak Werkstoff GmbH, Germany. The composite billets of ∅300 mm were machined to ∅297 mm and then extruded using an eightfold die to ∅30 mm bars at a deformation ratio of 12. The bars were cut into 50 mm long sections and extruded into strips of different thickness at Oxford University, using the parameters shown in Table 1.

### 2.2. Accumulative roll bonding (ARB)

ARB was conducted at the University of Buenos Aires using 1 mm thick strip already deformed to a true strain of  $\sim 6.1$ . Sample preparation involved strip degreasing in acetone and automatic sand brushing the faces to be bonded to remove any oxides. Both ends of the strips were fixed tightly together by stainless steel wire. ARB was carried out at room temperature and without lubrication, with a reduction in thickness of 50% per cycle (von Mises equivalent strain of 0.8). The roll diameter was 232 mm and the speed was 2 m/min. Any cracks generated at the strip edges were removed between each cycle. A total of 3 ARB cycles were carried out to a total true strain of  $\sim 8.4$ .

### 2.3. Sample preparation

Metallographic as spray formed, extruded and rolled samples were prepared by: (1) hot mounting sections of interest in a Poly-Fast phenolic resin; (2) grinding using 320 grit SiC paper; (3) polishing using MD-Plan cloths with a  $9 \mu\text{m}$  diamond suspension; (4) polishing using MD-Dur and MD-Chem cloths with colloidal silica + 10% hydrogen peroxide suspension. Thin foils from the extruded 1 mm strip of  $<200 \text{ nm}$  were machined from bulk using a FEI 200 focused ion beam microscope and placed on a carbon coated Cu grid for transmission electron microscopy (TEM) study. In order to investigate the 3D morphologies of the Ti and Si phases after extrusion and ARB, the Al matrix was dissolved using butanol according to Simensen et al. (1984), followed by filtering. The Ti and Si phases remained intact on the filter paper and were dried and studied in the secondary electron microscope (SEM).

### 2.4. Microstructural characterisation

SEM and electron backscattered diffraction (EBSD) analyses were carried out using a field emission gun JEOL 6500 SEM operating at 15 keV for secondary or backscattered electron imaging, and at 20 keV for EBSD data acquisition with samples tilted at  $70^\circ$  relative to the incident electron beam. EBSD scans were performed in a hexagonal scan pattern with a scan step size optimised for each magnification. An EDX TSL OIM acquisition system and analysis software was used for grain size and texture measurements.

A grain was defined as having at least three data points in order to remove inaccuracies associated with the measurement of grains with very few data points (Humphreys, 2001). The development of texture was also studied by X-ray diffraction (XRD) on sections along and transverse to the extrusion direction in a Siemens D5000 diffractometer operating with Cu K $\alpha$  X-ray of  $1.5406 \text{ \AA}$  wavelength.

### 2.5. Mechanical testing

Extruded strips were machined to an ASTM E8M (sub-size) tensile specimen and tests at ambient temperature were carried out at a cross-head speed of 0.5 mm/min, corresponding to a nominal strain rate of  $8.3 \times 10^{-4} \text{ s}^{-1}$ . The tensile direction was parallel to the extrusion direction.

## 3. Results and discussion

### 3.1. As-spray formed microstructure

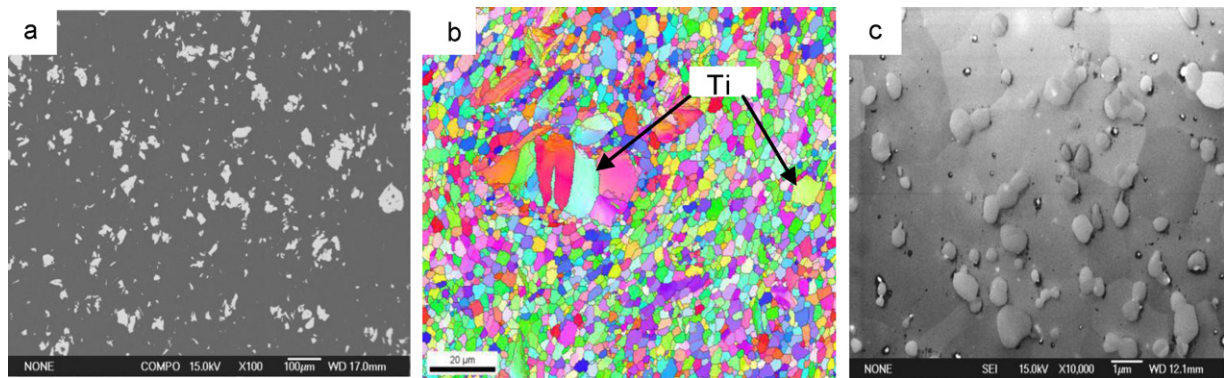
During co-spray forming, the commercially pure Ti particles were injected into the atomised Al–Si droplet spray through a separate set of gas jets close to the point of atomisation. The Ti powder mixed with Al–Si alloy droplets primarily during atomisation of the Al–Si melt stream and co-deposited into the billet with Ti particles uniformly distributed in the Al–Si matrix, as shown in Fig. 1a. The as-sprayed alloy composition was shown by chemical analysis to be close to the nominal composition, together with 0.13Fe.

The Ti particles had an irregular shape typical of manufacture by hydride–dehydride (HDH) process. There was no obvious clustering or banding as reported in co-spray formed Al–SiC<sub>p</sub> composites (Grant et al., 1995). Fig. 1b and c shows that the Al–Si matrix consisted of equiaxed  $\alpha$ -Al grains  $2\text{--}5 \mu\text{m}$  in diameter and a large number of Si particles of  $<1 \mu\text{m}$  diameter. The Si particles were often at the  $\alpha$ -Al grain boundaries and were formed during a fully divorced eutectic reaction at  $577^\circ\text{C}$ , as previously reported in sprayed eutectic (Baik and Grant, 1999) and hyper-eutectic Al–Si binary alloys (Hogg et al., 2006), and completely replacing the conventionally cast Al–12Si regular/irregular eutectic lamellar structure (Flemings, 1976). The removal of typically over 50% latent heat prior to deposition of the droplets (Mi and Grant, 2008) created a huge number of droplets containing solid Al dendrites that subsequently underwent copious fragmentation and remelting (Grant, 2007) at deposition. The fragmented Al dendrites provided an intrinsic  $\alpha$ -Al grain refining effect. Thus the as-spray formed microstructure comprised an unusual hierarchy of Si particles of  $<1 \mu\text{m}$ , a dilute  $\alpha$ -Al matrix of grain size  $2\text{--}5 \mu\text{m}$ , and Ti particles with  $D_{50} = 80 \mu\text{m}$ .

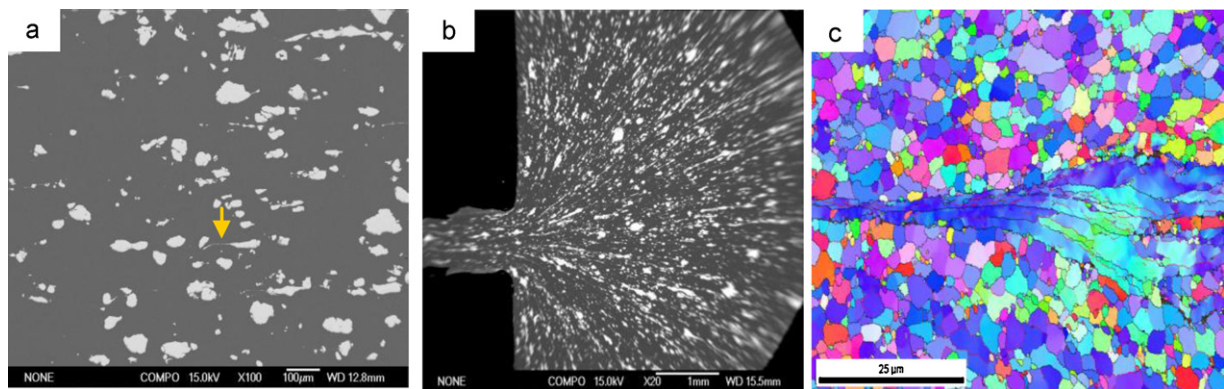
### 3.2. Extruded microstructure

Fig. 2a shows the microstructure of an extruded ∅30 mm bar with the majority of the Ti particles slightly deformed and elongated along the extrusion direction (ED). Only a small fraction of the Ti particles underwent significant deformation and formed very thin fibres of a few microns thickness, as highlighted by the arrow in Fig. 2a. Fig. 2b is a SEM image showing the deformation imposed on the Ti during extrusion through a 1 mm die. Fig. 2c shows an EBSD orientation map of the 2.5 mm strip, with a single elongated polycrystalline Ti particle.

Fig. 3 shows XRD traces comparing as-spray formed Al–12Si + 12Ti with the extruded 1 mm strip. There was slight  $\langle 111 \rangle$  texture in the  $\alpha$ -Al in the as-spray formed condition, due to a billet axial temperature gradient during final solidification (Hogg et al., 2006), and no texture in the Si or Ti. In the 1 mm thick strip and consistent with the EBSD data, there was again no strong texture in  $\alpha$ -Al, Si or Ti. Although conventional Al alloys often



**Fig. 1.** (a) Backscattered electron image of as-spray formed Al-12Si + 12Ti showing the morphology of Ti particles and their uniform distribution in the  $\alpha$ -Al; (b) an EBSD orientation map showing polycrystalline Ti particles and  $\alpha$ -Al grains; (c) secondary electron image showing the Al grains and divorced eutectic Si particles, primarily at  $\alpha$ -Al grain boundaries.



**Fig. 2.** (a) Backscattered electron image of extruded Al-12Si + 12Ti Ø30 mm bar showing slightly elongated Ti particles; (b) backscattered image showing the extrusion of Al-12Si + 12Ti through a rectangular 1 mm slot die; (c) an EBSD orientation map of a 2.5 mm strip showing fine  $\alpha$ -Al grains and a deformed Ti particle.

develop a strong (111) or other  $\alpha$ -Al texture during extrusion, texture development in spray formed and extruded hypereutectic Al-Si alloys studied in detail by X-ray pole figure analysis has previously been shown to be weak, even after an extrusion reduction of ~70% (Santos et al., 2005). We propose that particle stimulated nucleation (PSN) of dynamic recrystallization in Al-12Si due to the high number of ~1  $\mu$ m hard Si particles may have relieved accumulated strain energy and undermined the development of a pronounced sub-grain structure and macro-texture (Humphreys,

1977). The  $\alpha$ -Al grain size in this study was largely insensitive to the extent of deformation suggesting that PSN of recrystallization in the dilute  $\alpha$ -Al (limited/no solute drag) by the Si was comparatively easy at all stages of processing. It would be logical to produce a similar co-sprayed billet without Si particles to assess their role, for instance using unalloyed Al or a dilute solid solution. However, Al-12Si was chosen as a proof-of-principle deliberately due to its low melting point of ~577 °C that successfully minimised any reaction with Ti particles, which is a strong exothermic reaction to form various titanium aluminides. Given the early promise reported here, safe protocols for more dilute, higher melting point co-sprayed Al-based billet are currently under investigation.

Fig. 4a shows that for a 1 mm strip, over 50% of the Ti particles were deformed into fibres of thickness 0.5–2  $\mu$ m. Fig. 4b shows Si particles a few microns apart producing indentations and kinks along a deforming Ti fibre. TEM observations in Fig. 4c confirmed that unlike the  $\alpha$ -Al that was easily recrystallized, the Ti fibres accumulated a comparatively high dislocation density. There was no discernible Al-Ti interfacial reaction nor interfacial oxide at any of the magnifications used in the TEM studies.

### 3.3. Mechanical properties

At a total strain of 6, the yield stress of Al-12Si + 12Ti increased by over 30% relative to the extruded 30 mm bar with a strain of 2.5, with no loss of elongation to failure of 17%. This was still a relatively low total strain and fraction of Ti in comparison with small batches of powder processed Al-20 vol%Ti with strains >10 that showed dramatic strengthening (Russell et al., 1999): because the matrix/fibre interface acts as a barrier to dislocation (slip) propa-

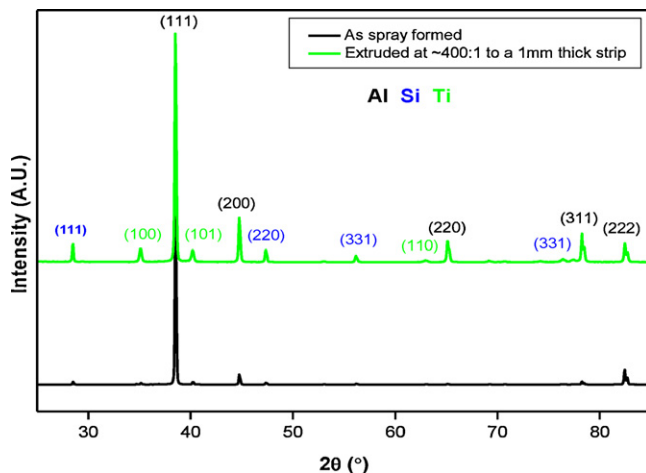


**Fig. 3.** XRD patterns comparing the as-sprayed Al-12Si + 12Ti material to the extruded 1 mm strip showing that only weak (111)  $\alpha$ -Al texture was induced after deformation to a strain of ~6.



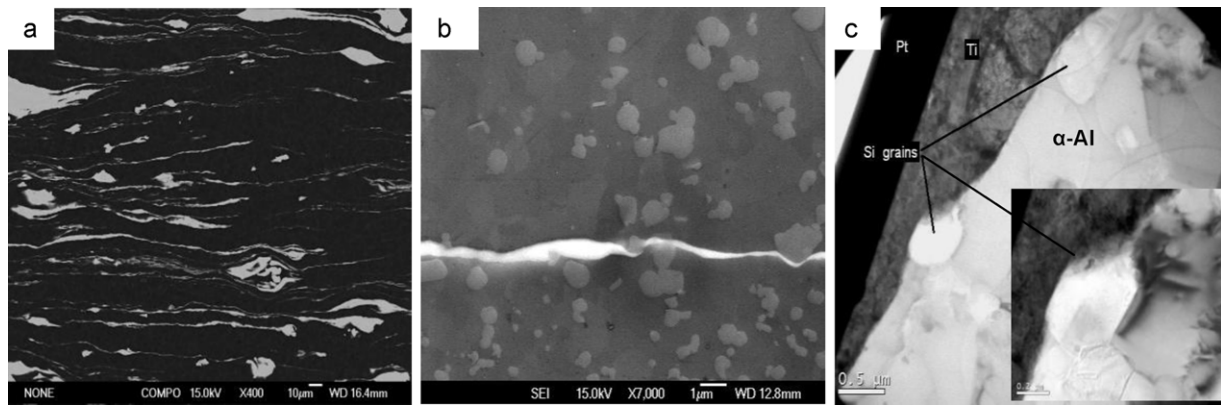


**Fig. 4.** (a) Backscattered electron image of further extruded Al-12Si + 12Ti 1 mm strip showing heavily elongated Ti; (b) secondary electron image showing the interaction between Si particles and the elongated sub-micron Ti fibre; (c) TEM image of the  $\alpha$ -Al/Ti interface with embedded Si particles.

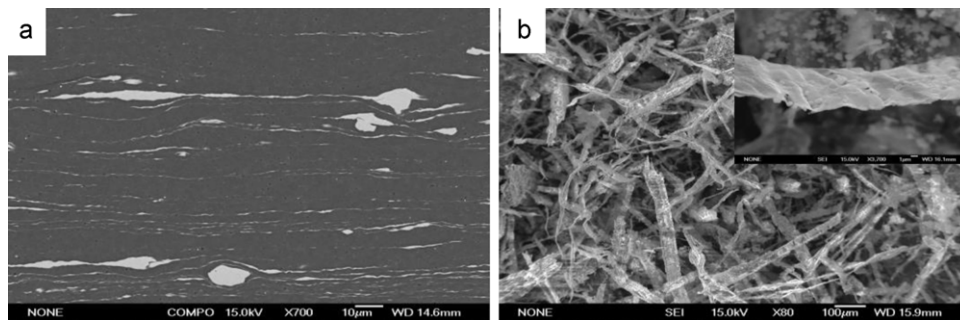


**Fig. 5.** (a) Backscattered electron image of ARB Al-12Si + 12Ti showing Ti fibres and ribbons of sub-micron thickness and (b) SEM image of Ti fibres and ribbons after dissolution of the  $\alpha$ -Al matrix.

**Table 2**

Mechanical properties of extruded 30 mm diameter bar and 1 mm thick strip (averaged over 3 measurements).

	Strain	Yield stress (MPa)	Elongation (%)
30 mm bar	2.5	94 ± 5	17 ± 0.6
1 mm strip	6.1	129 ± 1.5	17 ± 1

gation, strengthening is proposed dependent on the fibre spacing in a Hall–Petch type relationship (Spitzig et al., 1987). Nonetheless, these results provide encouragement for the feasibility of our spray forming based approach to scale-up (Table 2).

In order to assess the response of the material to higher strains, strips of 1 mm thickness were subjected to 3 ARB cycles resulting in a total true strain of  $\sim 8.4$ . The majority of Ti particles were reduced to sub-micron thickness as shown in Fig. 5a. There was no discernible fibre breakage, supporting previous ideas that the filamentary phase must be capable of a high recovery rate (Russell et al., 2000). Fig. 5b shows the Ti fibres after dissolution of the  $\alpha$ -Al matrix. Many Ti fibres or ribbons were now over 500  $\mu\text{m}$  long with thickness as small as a few hundred nanometers, although some only slightly deformed larger Ti particles remained, deriving from the large spread of Ti sizes in the starting powder. Due to removal of material at the edge of the strip, the final specimen size after 3 ARB cycles was too small for mechanical assessment.

#### 4. Conclusions

Spray forming with co-injection has been established as a new route to the manufacture of metal–metal composites at large scale. The Al-12Si + 12Ti industrial scale billet comprised refined equiaxed  $\alpha$ -Al grains ( $\sim 5 \mu\text{m}$ ), spherical Si particles ( $\sim 1 \mu\text{m}$ ) and uniformly distributed Ti particles ( $D_{50} = 80 \mu\text{m}$ ), and was free from

measurable interfacial reactions or oxides. Deformation processing was carried out to a true strain of  $\sim 8.4$  providing elongated Ti fibres of sub-micron thickness and  $\alpha$ -Al grains that underwent particle stimulated dynamic recrystallization due to the Si particles to maintain a fine, near-constant grain size irrespective of total strain. It is suggested that during deformation, the Si particles may have also played a role in imparting stress to the Ti particles to produce fibres of sub-micron thickness. Preliminary tensile properties suggest that progressive Ti elongation provided modest strengthening. Larger Ti fractions and deformations are now being studied, with accumulative roll bonding proving to be an encouraging deformation processing route to scale-up.

#### Acknowledgements

The authors would like to thank the UK Engineering and Physical Science Research Council (Grant EP/E040608/1) for financial support, and Dr. K. Jurkschat and Dr. A. Lui of Oxford University for their assistance with TEM and phase extraction, respectively.

#### References

- Baik, K.H., Grant, P.S., 1999. Microstructural evaluation of monolithic and continuous fibre reinforced Al-12 wt%Si produced by low pressure plasma spraying. *Materials Science and Engineering A* 265, 77.
- Bevk, J., et al., 1978. Anomalous increase in strength of *in situ* formed Cu–Nb multifilamentary composites. *Journal of Applied Physics* 49, 6031.
- Flemings, M., 1976. *Solidification Processing*. McGraw-Hill, New York.
- Grant, P.S., et al., 1995. Spray forming of Al/SiC metal matrix composites. *Journal of Microscopy* 177, 337–346.
- Grant, P.S., 2007. Solidification in spray forming. *Metallurgical Transactions A* 38, 1520.
- Hogg, S., et al., 2006. Microstructural characterisation of spray formed Si-30Al for thermal management applications. *Scripta Materialia* 55, 111–114.
- Humphreys, F.J., 1977. The nucleation of recrystallization at second phase particles in deformed aluminium. *Acta Metallurgica* 25, 1323–1344.

- Humphreys, F.J., 2001. Review: grain and subgrain characterisation by electron backscatter diffraction. *Journal of Materials Science* 36, 3833–3854.
- Mi, J., Grant, P.S., 2008. Modelling the shape and thermal dynamics during the spray forming of Ni superalloy rings. Part 1. Droplet deposition, splashing and re-deposition. *Acta Materialia* 56, 1588–1596.
- Russell, A.M., et al., 1999. A high-strength, high-conductivity Al–Ti deformation processed metal matrix composite. *Composites Part A* 30, 239–247.
- Russell, A.M., et al., 2000. Review: deformation processed metal–metal composites. *Advanced Engineering Materials* 2, 11–22.
- Saito, Y., et al., 1999. Novel ultra-high straining process for bulk materials—development of the accumulative roll-bonding (ARB) process. *Acta Materialia* 47, 579–583.
- Santos, H.O., et al., 2005. Crystallographic orientation of spray formed hypereutectic aluminium–silicon alloys. *Materials Research* 8, 181–186.
- Simensen, C.J., et al., 1984. Analysis of intermetallic particles in aluminium by dissolution of the sample in butanol. *Fresenius Zeitschrift Fur Analytische Chemie* 319, 286–292.
- Spitzig, W.A., et al., 1987. Characterization of the strength and microstructure of heavily cold worked Cu–Nb composites. *Acta Metallurgica* 35, 2427–2442.
- Thieme, C.L.H., et al., 1993. High strength Al metal–matrix microcomposite wire with 20 vol% Nb and ultimate tensile strengths up to 1030 MPa. *Scripta Metallurgica et Materialia* 28, 913–918.